Cardiac MRI at 3T: An Indian Experience of 80 Cases of Cardiac MRI with Review of Literature

Kalashree A. Bidarkar DNB; Nikhil Kamat, M.D., DMRD, DNB; M. L. Rokade, M.D., DNB; Nitin Burkule, M.D., DM; Shubra Gupta

Departments of Radiology and Cardiology, Jupiter Hospital, Thane, Maharashtra, India

Abstract

Diagnostic clinical cardiac magnetic resonance imaging (MRI) requires an appropriate combination of temporal and spatial resolution. Cardiovascular imaging is making considerable advances toward the fulfillment of these requirements, largely because of continued improvements in MRI hardware and software. Optimal diagnostic-quality MRI implies a balance among signal-to-noise ratio (SNR), tissue contrast, acquisition time, and spatial and temporal resolution. Magnetic field strength is one of the major factors affecting image SNR [3]. The transition from 1.5T to 3T has resulted in faster imaging and better SNR. However, cardiac MRI protocols on 3T have not yet been optimized in the way that they have been optimized for 1.5T over the last decade.

This article illustrates 80 cases of cardiac MRI imaged on a 3T MRI system (MAGNETOM Verio, 32-channel system) at our institution done between January 2012 and August 2013. This is probably the largest study of cardiac MRI done on a 3T in India.

Introduction

The role of magnetic resonance imaging (MRI) has significantly evolved over the last decade. MRI is now considered useful in the evaluation of pericardium, complex congenital heart disease, cardiac masses, and ischemic heart disease for myocardial viability, hibernating and stunned myocardium and the right ventricle.

In 2002, the US Food and Drug Administration's (FDA) approval of 3 Tesla opened the way for multiple clinical applications. Compared to 1.5T, the higher field strength results in doubling of SNR due to increased spin polarisation. Furthermore, imaging at higher field strengths with gadolinium-based agents can produce further improvements in image contrast. Cardiac imaging at 3T is, however, noticeably different from imaging at 1.5T because of a variety of artifacts that result from susceptibility effects and augmentation of radiofrequency (RF) inhomogeneity [3].

The adoption of 3T for body applications, especially cardiac applications, has been somewhat slower. The slower acceptance of 3T for cardiac applications is due to the unique challenges posed by cardiac imaging: Requirement of a large field-of-view, the motion of the heart, position of the heart within the body, proximity of heart to the lungs, and high RF power deposition required in many fast cardiac imaging sequences [1]. Cardiac MRI has largely been done on a 1.5T in

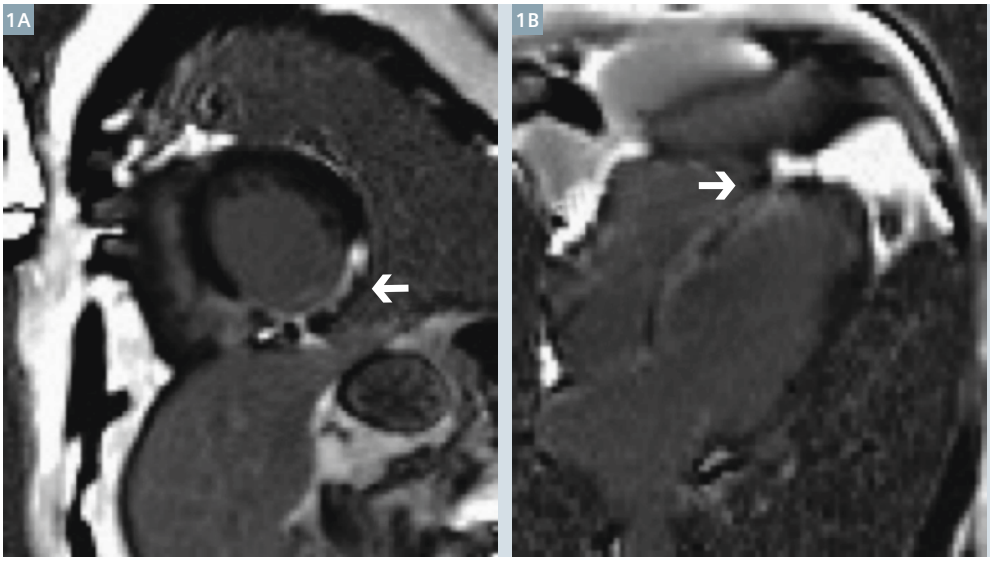

1A

68-year-old male patient imaged for evaluation of myocardial viability. PSIR sequence taken 15 minutes post Gd administration reveals transmural LGE in the inferior wall conforming to RCA and the LCX territory (solid white arrows) suggestive of non-viable myocardium.

1B

Horizontal long axis view of the same patient showing the extent of transmural LGE.

India. Due to optimization done on 1.5T and apprehension of challenges on a 3T system, no significant work was done on 3T in India. We present probably the largest number of cardiac MRI cases performed till date on a 3T in India.

There are several advantages which motivate users to perform cardiovascular magnetic resonance (CMR) at higher filed strengths. First, the bulk magnetisation increases as the magnetic field strength is increased resulting in higher SNR. Second, the increasing field strength increases the frequency separation of off-resonance spins. The enhanced frequency differences may be exploited for improvement in spectroscopic imaging and potentially in fat suppression. A third advantage is increased T1 signal of many tissues, resulting in beneficial effects in some applications, such as myocardial tagging and myocardial perfusion sequences [1].

Methods and Materials

A) Patient population

Eighty patients with an age range of 5 to 70 years with a suspected cardiac pathology were evaluated by cardiac MRI (CMR) at our institute from January 2012 to August 2013. All patients had undergone a prior echocardiography.

B) Patient preparation

A detailed history was elicited from each patient including principal symptoms and signs, echocardiographic and cardiac catheterisation data. For all patients in this study, MR compatible electrocardiographic leads were placed in the anterior chest wall before imaging and attached to the MR imaging unit for electrocardiographic gating. For most sequences, electrocardiographic triggering was used to synchronise imaging with the onset of systole and offset cardiac motion and match each image to the desired cardiac phase.

C) Cardiac MRI protocol

Cardiac MRI was performed using a whole-body 3T scanner (MAGNETOM Verio, Siemens Healthcare, Erlangen, Germany). MR imaging protocol commenced with a localiser using TrueFISP (steady-state free precision) sequence. A list of protocols is given in table 2. Axial and coronal scans of 5 mm slice thickness were obtained from the aortic arch to diaphragm. All diagnostic sequences were acquired in standard angulations (4-, 2-chamber view and short axis) using a matrix of at least 256 × 256. Myocardial function was evaluated by cine TrueFISP sequences; T2-weighted dark blood turbo spin echo sequences were acquired 5 and 15 minutes after injection of 0.15 mmol gadolinium diethylene triamine penta-acetic acid (DTPA) (Magnevist, Schering, Berlin, Germany) per kilogram of body weight.

Inversion recovery prepared turbo sequences (FLASH and TrueFISP) were performed to visualise the myocardial and blood pool gadolinium kinetics, and to adjust inversion time. An inversion time (TI) scout was acquired and the optimal TI value was found. Endocardial counters of the left ventricle were manually drawn using dedicated software (Argus, Siemens Healthcare, Erlangen, Germany) to calculate end-diastolic volume, end-systolic volume, stroke volume and ejection fraction of the left ventricle [8]. In the case of evaluation of congenital heart diseases, scans were obtained till below the diaphragm including IVC and the hepatic veins [23].

A summary of the basic cardiac protocols is presented in table 1.

Modified sequences were acquired for specific indications which have been summarised in table 2.

D) Results

The study comprised 80 patients. The age range was 5 to 70 years. There were 57 male and 23 female patients. The commonest indication for a CMR study was evaluation of myocardial viability.

The variety of indications for which cardiac MRI was performed is summarised in table 4.

Images were analysed by one radiologist and one cardiologist. The morphological information comprised of chamber anatomy, thickness of the ventricular walls and assessment of presence and extent of late gadolinium hyper-enhancement on delayed post contrast PSIR images.

Functional information comprised of assessment of wall motion abnormalities, calculation of ejection fraction and evaluation of the outflow tracts.

In cases of congenital heart disease, cine imaging in horizontal long axis provided dynamic information of the cardiac size, valve morphology, wall thickness chamber size, and septum morphology and aortopulmonary connections [23].

55 patients were referred for evaluation of myocardial viability. Of these, 30 showed transmural late gadolinium enhancement (LGE) in

Table 1: MR sequencing

Anatomy	HASTE 2D
Function	Cine SSFP (2CV,4CV,SA)
Morphology	T1-weighted (2CV,4CV,SA) STIR dark blood (2CV,4CV,SA)
Fluid content	T2-weighted (2CV,4CV,SA)
Gadolinium kinetics	TI scout baseline
Delayed enhancement	IR turbo TrueFISP 2D

Abbreviations: 2D, 2 dimensional ; CV, chamber view; IR, inversion recovery; SA, short axis; TI, inversion time; STIR, Short TI Inversion Recovery; TSE, turbo spin echo

Table 2: Special considerations

Acute MI	T2-weighted or STIR dark blood
Cardiac mass or thrombus	TSE dark blood T1, TSE dark blood T2 fat sat

the LAD, 10 in the RCA and 4 in the LCX territories, corresponding to non-viable myocardium (Table 3).

11 patients demonstrated < 50% of myocardial LGE. Of these, 5 belonged to LAD territory and 2 and 4 to the LCX and RCA territories, respectively (Table 3).

On follow up, 7 patients underwent revascularisation procedures. All of these reported to experience symptomatic relief.

15 patients were evaluated for cardiomyopathy. All patients with CMP are managed by medical therapy and are doing well.

We evaluated 2 patients for constrictive pericarditis. Both were started on anti-Koch's therapy and are symptomatically better.

5 patients were referred for evaluation of cardiac masses after an echocardiographic study. 3 of these had revealed a LV clot and 1 patient had demonstrated a nodular mass attached to the LV wall. One patient suspected to have a mass posterior to left atrium on echocardiography was diagnosed with straight back syndrome with the thoracic vertebral body indenting the left atrium. LV clots were confirmed on CMR and the patients were put on anticoagulation therapy.

One patient diagnosed as LV myxoma being managed on medical therapy, is doing well.

Table 3

Transmural extent	LAD	LCX	RCA
> 50%	30	4	10
< 50%	5	2	4

Table 4

Indications	Number of patients
1) Myocardial viability	55
2) Recent MI	2
3) Cardiomyopathies	15
a) Hypertrophic cardiomyopathy	8
b) Dilated cardiomyopathy	5
c) Non compaction cardiomyopathy	2
d) Restrictive cardiomyopathy	1
4) Cardiac masses	5
5) Congenital heart disease	1
6) Pericardium (constrictive pericarditis)	2

Discussion

A) Myocardial viability

Ischemic heart disease (IHD) is today one of the leading causes of death all over the world. Cardiac MRI plays an important role complementary to other imaging modalities in evaluation of patients with IHD. Myocardial infarction results from rupture of an atherosclerotic plaque in a coronary artery leading to thrombus formation. The subendocardium is most vulnerable to ischemia and an infarct expands form subendocardium to subepicardium [7].

Myocardial infarction, scarring and viability are simultaneously examined using technique of delayed enhancement MRI.

Delayed / late gadolinium hyperenhancement is caused by delayed washout of contrast agent from the myocardium. Delayed enhancement is performed 10–15 minutes after i.v. administration of 0.15 to 0.2 mmol/kg of gadolinium. An inversion recovery sequence is used in which normal myocardium is nulled to accentuate the delayed enhancement [7].

Both acute and chronic infarctions enhance. In acute infarctions, contrast enters the damaged myocardial cells due to membrane disruption (microvascular obstruction / no reflow zones). These regions are recognised as dark central areas surrounded by hyperenhanced necrotic myocardium. This finding indicates the presence of damaged microvasculature in the core of an area of infarction. The presence of a 'no-reflow' zone appears to be associated with worse LV remodelling and outcome [7, 9]. CMR can be safely carried out in patients with acute MI and primary angioplasty and aids in risk stratification. T2-weighted imaging allows the detection of myocardial edema, allowing for early diagnosis of myocardial ischemia, area at risk, and salvage [22] (Fig. 4).

In chronic infarctions, the LGE is a result of retention of contrast medium in large interstitial space between collagen fibres in the fibrotic tissue.

Stunning and hibernating myocardium

Cine imaging in combination with delayed enhancement MRI allows identification of:

1) ***Myocardial stunning:*** Stunning is defined as post-ischemic myocardial dysfunction (seen in the setting of acute myocardial ischemia) which persists despite restoration of normal blood flow. Over time there can be a gradual return of contractile function depending on transmurality of the ischemia. If the degree of transmurality as seen on delayed enhancement images is < 50%, the myocardial function is likely to recover.

2) ***Hibernating myocardium:*** A state in which some segments of the myocardium exhibit abnormalities of contractile function at rest. This phenomenon is clinically significant since it manifests in the setting of chronic ischemia that is potentially reversible by revascularisation. The reduced coronary perfusion causes the myocytes to enter into a low energy 'sleep mode' to conserve energy. There is an inverse relationship between transmural extent of hyperenhancement, and likelihood of wall motion recovery following revascularisation [5].

Multiple experimental studies have demonstrated excellent spatial correlation between the extent of hyperenhancement and areas of myocardial necrosis (acute MI) or scarring (chronic MI) at histopathology.

Specifically, there is an inverse relationship between transmural extent of hyperenhancement and likelihood of wall motion recovery following revascularisation. Hence it follows that myocardial regions which show little or no evidence of hyper-enhancement (i.e. infarction) have a high likelihood of recovery, whereas regions with transmural hyperenhancement have virtually no chance of recovery [9].

Moving from a 1.5T to a 3T system involves doubling of SNR which can be used to increase either spatial or temporal resolution. This translates into potentially increased contrast between perfused and non-perfused images leading to increased contrast-to-noise ratio (CNR) with better LGE in setting of chronic ischemia [1].

Figures 1–3 demonstrate LGE in the RCA & LCX, LCX and LAD territories, respectively, significant other non-viable myocardium in these regions.

Diagram 1 [7]: A schematic representation of three zones of affection in case of an MI:

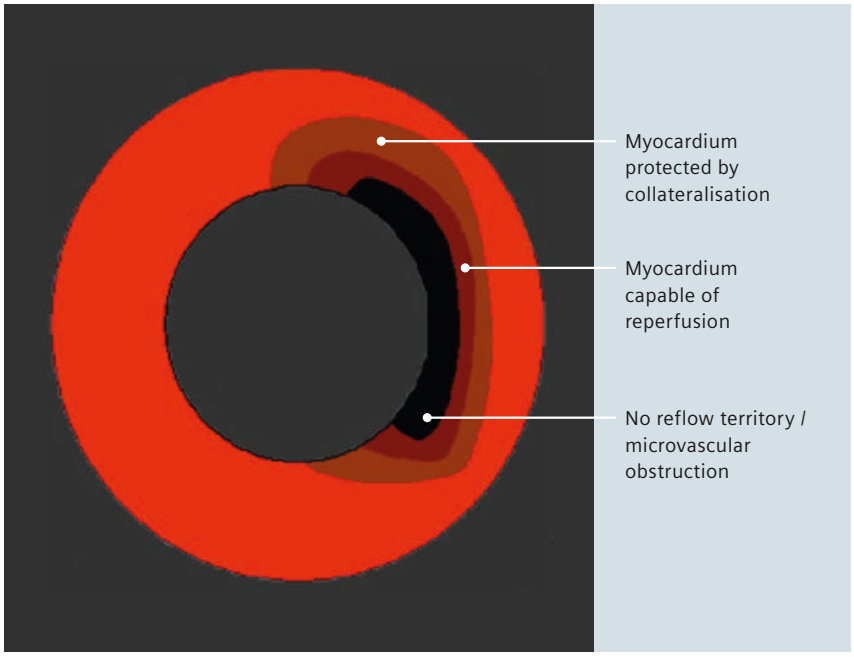

Table 5 [9]: Differentiation between acute and chronic MI.

Acute MI	Chronic MI
Bright on pre-contrast STIR (or T2w) imaging	Not bright on pre-contrast STIR(or T2w) imaging
Walls may be thicker than usual	Walls may be thinned
May have a 'no-reflow zone'	Does not have a 'no-reflow zone'

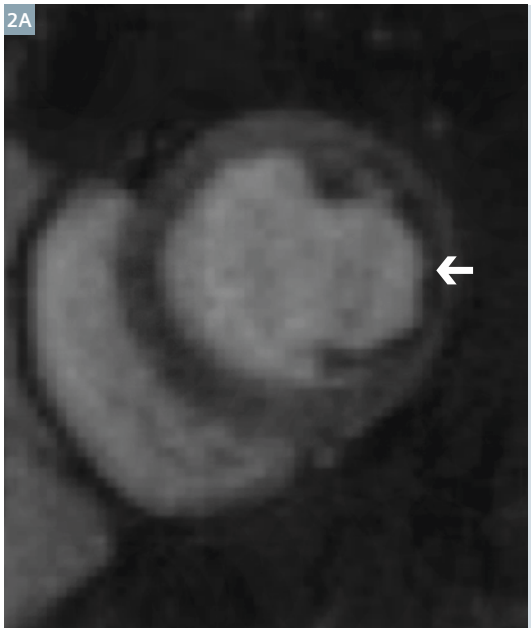

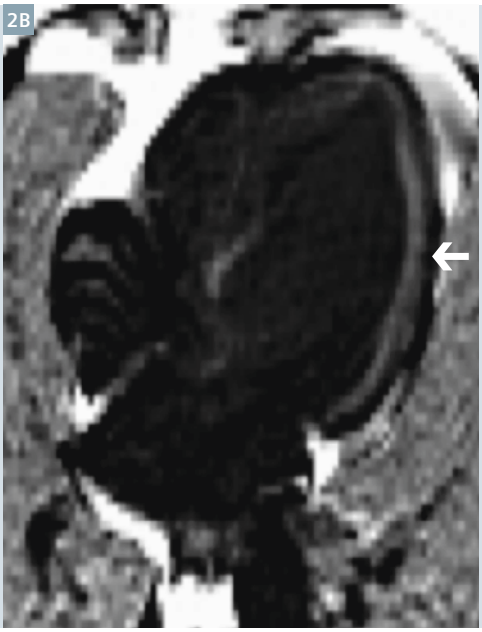

2A

PSIR short axis image acquired immediately post Gd administration in a 60-year-old female patient reveals subendocardial 1st pass defect in the lateral wall (solid white arrow).

2B

PSIR images taken 15 minutes after Gd administration reveal subendocardial LGE with transmural extent suggestive of non-viable myocardium in the LCX territory (solid white arrow).

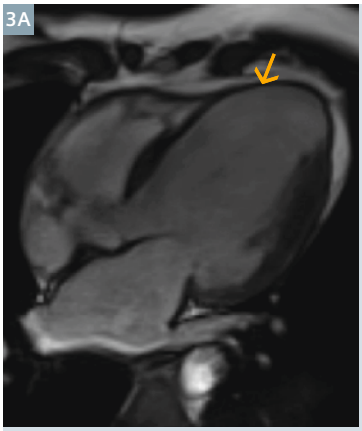

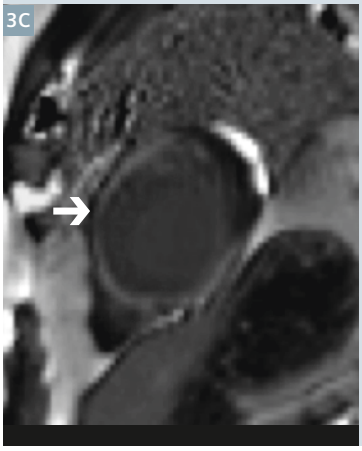

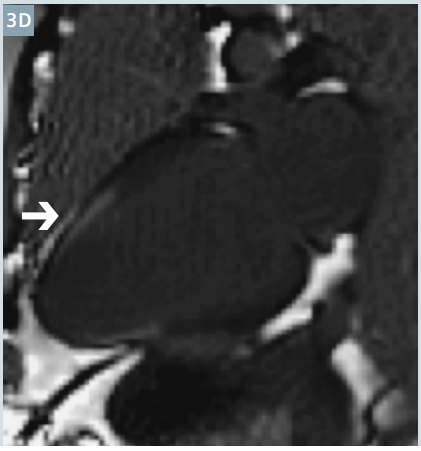

3

3A, B, 4C, 2C views reveal moderate dilated LA and LV with thinning of LV anterior wall, interventricular regions and the apex. Aneurysmal dilatation of the thinned apex is seen (thin yellow arrows).

(3B, C) PSIR images taken 15 minutes post Gd administration reveal transmural LGE in these (solid white arrows) areas suggestive of non-viable myocardium in the LAD territory.

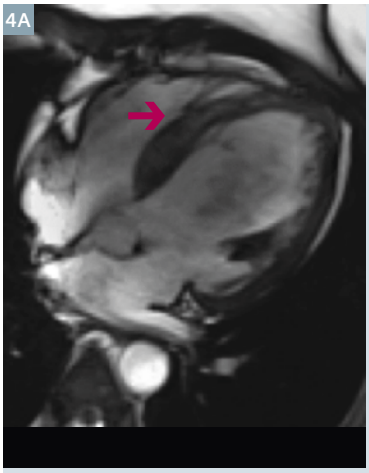

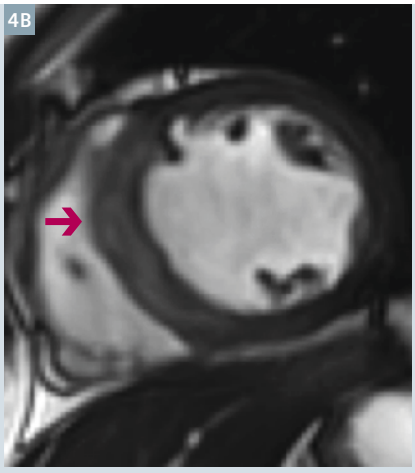

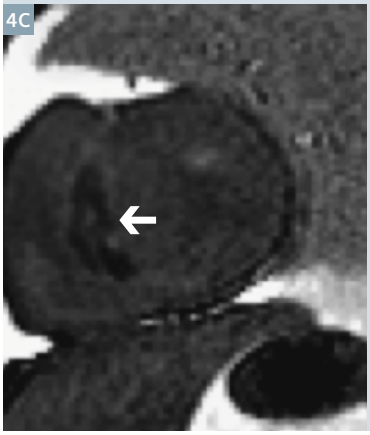

4

42-year-old male patient with symptoms of acute myocardial infarction.
(4A, B) SSFP 4-chamber and short axis images reveal mildly thickened interventricular septum with subtle hyperintense areas suggestive of post-MI edema (solid red arrows).

(4C, D) PSIR images acquired immediately post Gd administration demonstrate perfusion defect in the LAD territory corresponding to microvascular obstruction (solid white arrows).

Figure 4 demonstrates CMR findings in acute myocardial infarction, seen as edema on T2-weighted images and perfusion defect (microvascular obstruction) on the post-contrast PSIR images.

B) Pericardium

MRI is particularly suitable for evaluation of pericardial inflammation, evaluation of small or loculated pericardial effusions, functional abnormalities caused by pericardial constriction, and for characterization of pericardial masses [19].

The diagnosis of constrictive pericarditis is greatly aided by excellent depiction of pericardium at MR imaging. Normal pericardium is less than 3 mm thick. Pericardial thickness of 4 mm or more indicates abnormal thickening, and when accompanied by clinical signs of heart failure is highly suggestive of constrictive pericarditis [10]. Pericardial thickening may be limited to the right side of the heart or even a smaller area such as the right atrio-ventricular groove.

In chronic constrictive pericarditis there is typically bi-atrial enlargement. Also, the central cardiovascular structures show a characteristic morphology with the right ventricle showing a narrow tubular configuration [10].

Cine images are useful to judge the pathophysiologic consequence of pericardial thickening and the 'Diastolic Septal bounce' [7].

Diastolic septal bounce is a hemodynamic hallmark of ventricular constriction seen due to increased interventricular dependence and demonstrated as abnormal ventricular septal

motion towards the left ventricle in early diastole during onset of inspiration [9]. This finding is helpful in distinguishing between constrictive pericarditis and restrictive cardiomyopathy [9] (Fig. 6).

Figure 5 illustrates the characteristic findings of thickened pericardium and diffuse pericardial enhancement in a case of constrictive pericarditis.

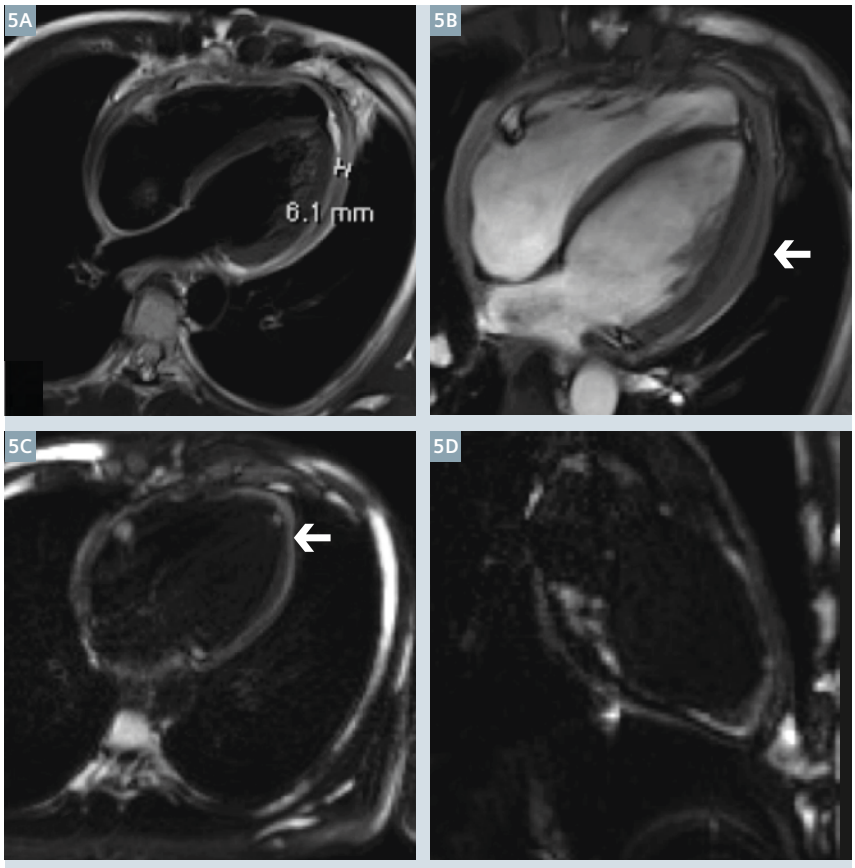

5 35-year-old male patient on treatment for pulmonary Koch's disease, presented with dyspnoea.
(5A, B) Horizontal long axis black and white blood images reveal thickened pericardium (6 mm).
(5C, D) Post-contrast images acquired 15 minutes post Gd administration reveal diffuse pericardial enhancement consistent with the diagnosis of constrictive pericarditis.

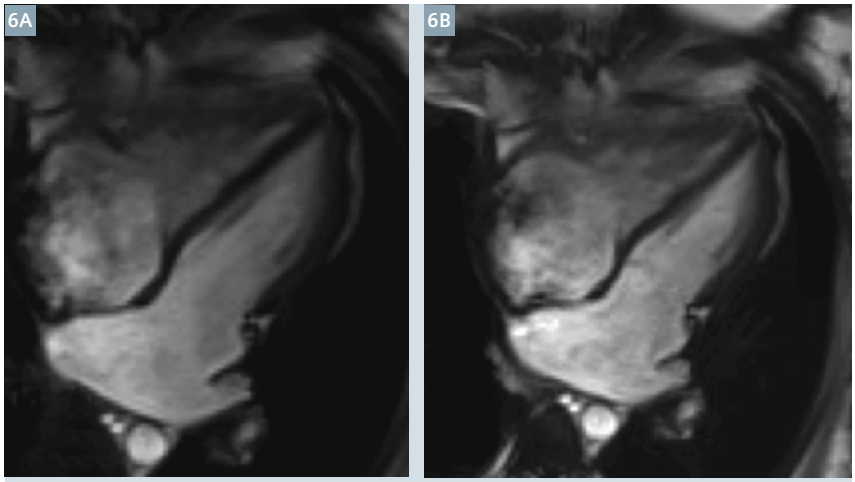

6 An example of Diastolic septal bounce. Septal flattening / inversion seen in constrictive pericarditis, since outward expansion of the right ventricle is limited by a non-compliant pericardium.
(6A) Shows IV septum in mid systolic phase.
(6B) Diastolic phase reveals mild leftward bowing of the septum.

C) Cardiomyopathies (CMPs)
Cardiomyopathies are chronic progressive diseases of the myocardium with often genetic / inflammation / injury as factors contributing to their development [7]. Cardiac MRI has become an important tool for the diagnosis and follow-up of patients with cardiomyopathies. It has a unique ability to differentiate between different enhancement patterns in diseased myocardium on inversion recovery delayed Gadolinium-enhanced images, making it suitable for evaluation of cardiomyopathies [18].

Hypertrophic cardiomyopathy (HCM): A genetically-acquired condition resulting from abnormality in the sarcomere, it results in hypertrophy of the myocardium.

MRI has proven to be an important tool in the evaluation of patients with suspected HCM since it helps readily diagnose those with phenotypic expression of the disorder and potentially identify the subset of patients at risk of sudden cardiac deaths. MRI is also capable of detecting regions of localised hypertrophy that are missed by echocardiography.

A significant percentage of patients with HCM demonstrate LGE characteristically involving regions of hypertrophy, junctions of interventricular septum and RV free wall [9]. LGE is usually patchy and midwall in location. LGE in HCM also has a predilection for the anterior and posterior insertion points. An exception to this is in areas of burnt-out myocardium where the left ventricular wall is thinned and enhancement is full thickness [18].

The presence of LGE denotes scar tissue, a potential nidus for fatal arrhythmias. CMR can be used to follow the patients following ventricular septal resection / percutaneous ablation [7].

Phenotypes of HCM

1) Asymmetric HCM
This is the most common morphologic presentation of HCM, the anteroseptal being the commonly hypertrophied segment. Asymmetric septal wall hypertrophy causes LVOT obstruction in 20–30% of cases.

Asymmetric / septal HCM may be diagnosed when septal thickness is greater than or equal to 15 mm or when the ratio of septal thickness to the thickness of inferior wall of the left ventricle is greater than 1.5 at the midventricular level [20].

Abnormalities of the mitral valve may occur due to primary abnormality of the valve itself or due to LVOT obstruction. Systolic anterior motion of the mitral valve (SAM) is a phenomenon in which a portion of the anterior leaflet of the mitral valve distal to the coaptation gets displaced / pulled in to the LVOT by venture or drag forces, leading to transient LVOT obstruction [7] (Fig. 9). Over time, the systolic anterior motion of the mitral valve leads to sub-aortic mitral impact lesion on the septum which undergoes fibrosis; thickening of mitral leaflet and chordae from the resultant trauma; a posteriorly directed mitral regurgitant jet in to the left atrium and a systolic gradient along the LVOT [18].

Patients with LVOT obstruction unresponsive to medical therapy (5%) are candidates for surgical myectomy or septal alcohol ablation [20]. Our patient, however, was put on medical therapy.

2) Apical HCM
The apical variant of HCM shows an absolute apical thickness of > 15 mm or a ratio 1.3 to 1.5. More subjective criteria are the obliteration of LV apical cavity in systole and failure to identify a normal progressive reduction in LV wall thickness towards the apex.

The left ventricle shows a characteristic 'spade-like' configuration on vertical long axis views.

An apical aneurysm formation with delayed enhancement is sometimes seen referred to as the 'burnt-out apex' resulting from ischemia due to reduced capillary density resulting in ischemic fibrosis. Similar appearance of 'burnt-out apex' is also seen in HCM causing mid- ventricular obstruction with apical aneurysm formation, as described in figure 8.

The LV apex may not be assessed well with echocardiography leading to false negative interpretations. Hence cardiac MRI is strongly recommended as optimal imaging modality for evaluation of apical HCM [20].

3) HCM with mid-ventricular obstruction
A variant of asymmetric HCM predominantly involving the middle third of the left ventricle may result in severe mid-ventricular narrowing and obstruction. This condition may be associated with formation of an apical aneurysm which is thought to result from increased generation of systolic pressures within the apex from the mid-ventricular obstruction [18] (Fig. 8).

4) Symmetric HCM
This variant is encountered in about 42% of HCM cases and is characterized by a concentric LV hypertrophy with a small cavity dimension and no evidence of a secondary cause. This entity has to be differentiated from other causes of diffuse LV wall thickening including athlete's heart, amyloidosis, sarcoidosis, Fabry's disease, and secondary adaptive pattern of LV hypertrophy due to hypertension or aortic stenosis, since the treatment strategies differ. Cardiac MRI is known to play an important role in differentiating other causes of myocardial hypertrophy from HCM because of the unique ability of DE MRI imaging to characterize different enhancement patterns in diseased myocardium [20]. Figure 7 illustrates a case of concentric HCM in a symptomatic patient.

5) Mass-like HCM
Mass-like HCM manifests as a mass-like hypertrophy because of focal segmental location of myocardial disarray and fibrosis which may be differentiated from neoplastic masses. MR imaging with first pass perfusion and DE technique helps to differentiate between the two

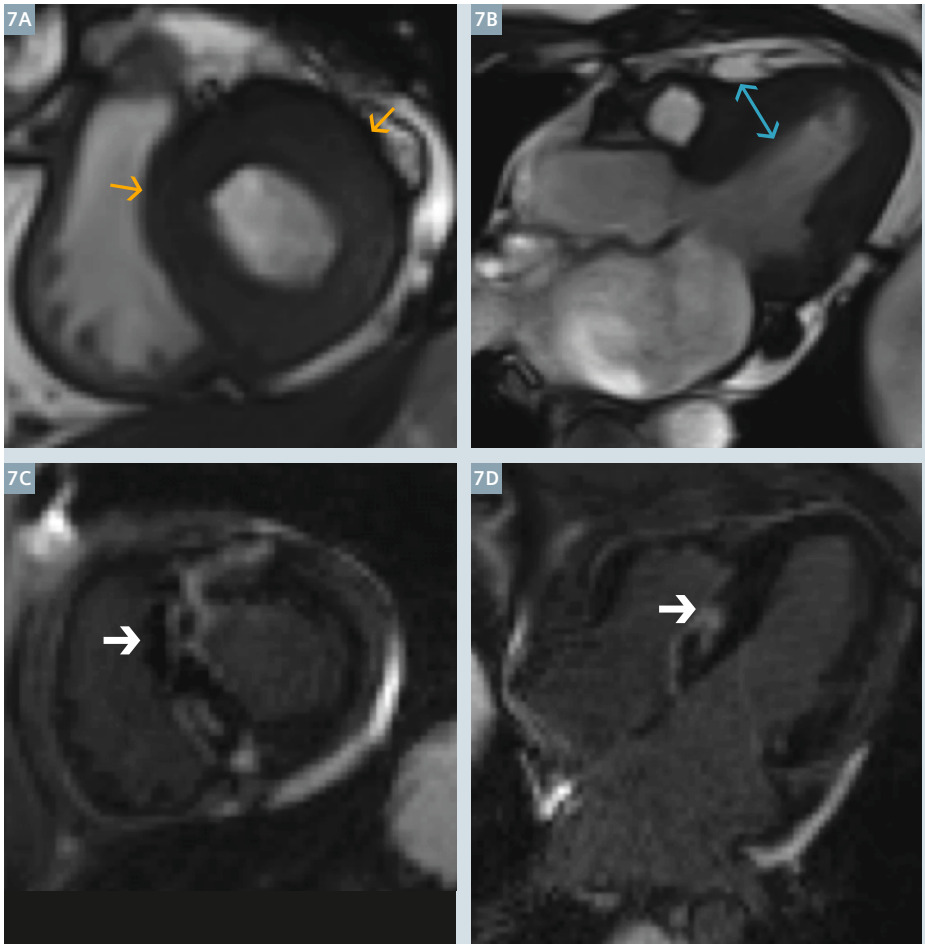

7

Concentric HCM in a symptomatic 35-year-old male patient.
(7A, B) Short axis and vertical long axis SSFP images show symmetrically thickened LV walls (arrows) with atrial dilatation.

(7C, D) PSIR images acquired 15 minutes post Gd administration reveal patchy transmural LGE in the thickened IV septum and RV insertion sites, suggestive of scarred tissue (solid white arrows).

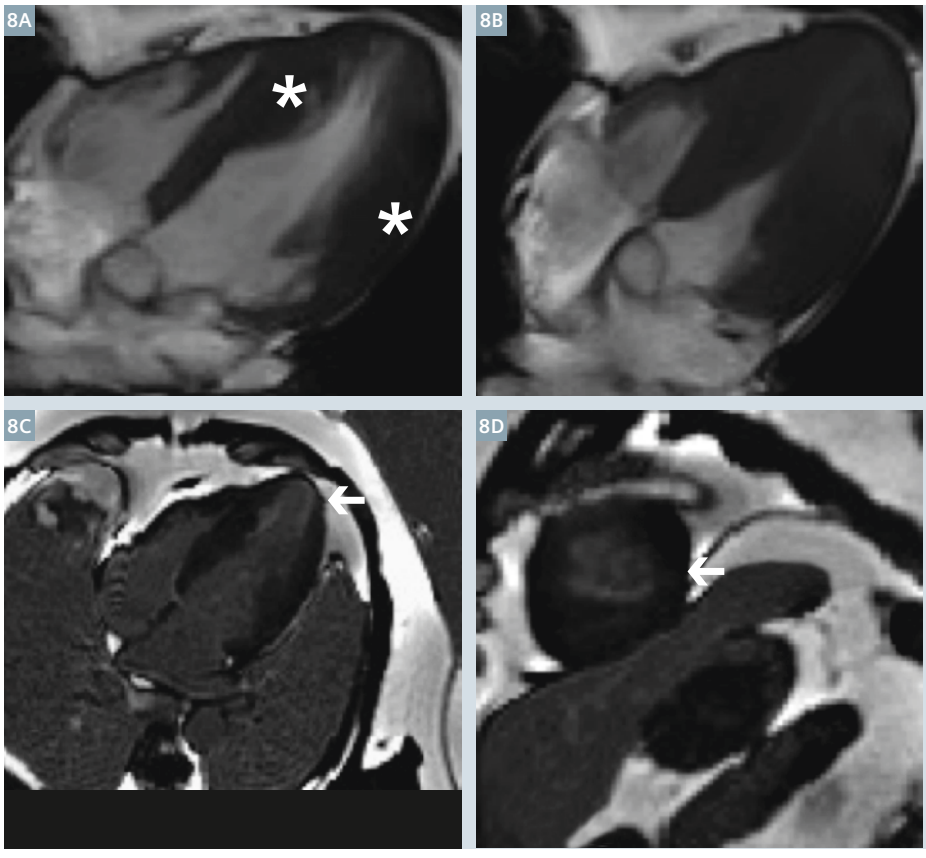

8

HCM with mid-ventricular obstruction. CMR evaluation of a 55-year-old male patient with a family history of sudden cardiac deaths.
(8A, B) Horizontal long axis SSFP cine MR images reveal significant hypertrophy of the LV myocardium (16–17 mm width). The thickened myocardium (asterisk in 8A) causes mid-cavity obstruction with apical thinning and outpouching resulting in a 'dumbbell shaped LV'.
(8C, D) PSIR images acquired 15 minutes post Gd administration show subendocardial LGE (solid white arrows), around 50% in the proximal areas and transmural in the apex (burnt out apex) suggestive of ischaemic fibrosis.

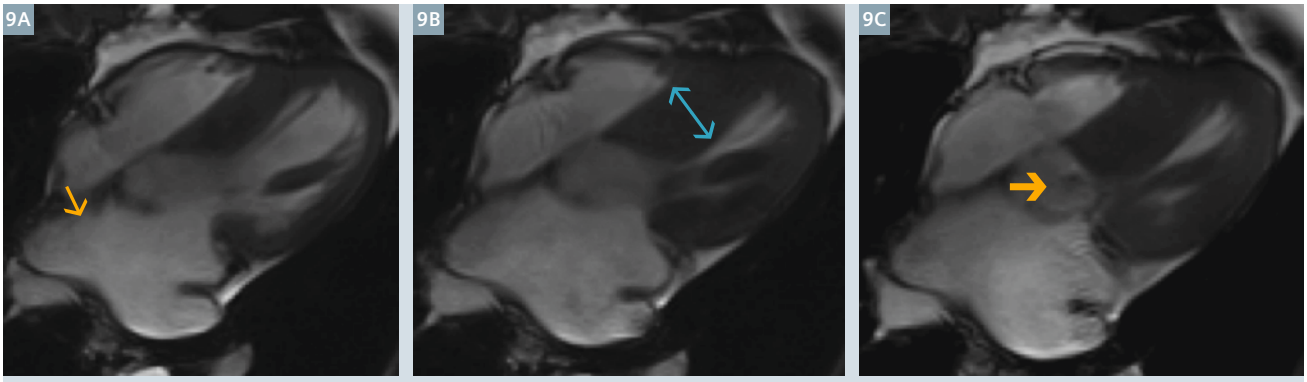

9 32-year-old male patient with a history of sudden atrial fibrillation was evaluated by CMR.
(9A, B) SSFP sequential 3-chamber SSFP cine MR images in the diastolic and mid-systolic phases respectively reveal LV hypertrophy (double headed arrow in 9B) and LA dilatation (thin yellow arrow).
(9C) Systolic phase demonstrates anterior motion of the mitral leaflet causing obstruction at the LVOT (solid yellow arrow) with resultant turbulent jets in the LA and at the LVOT – systolic anterior motion (SAM).

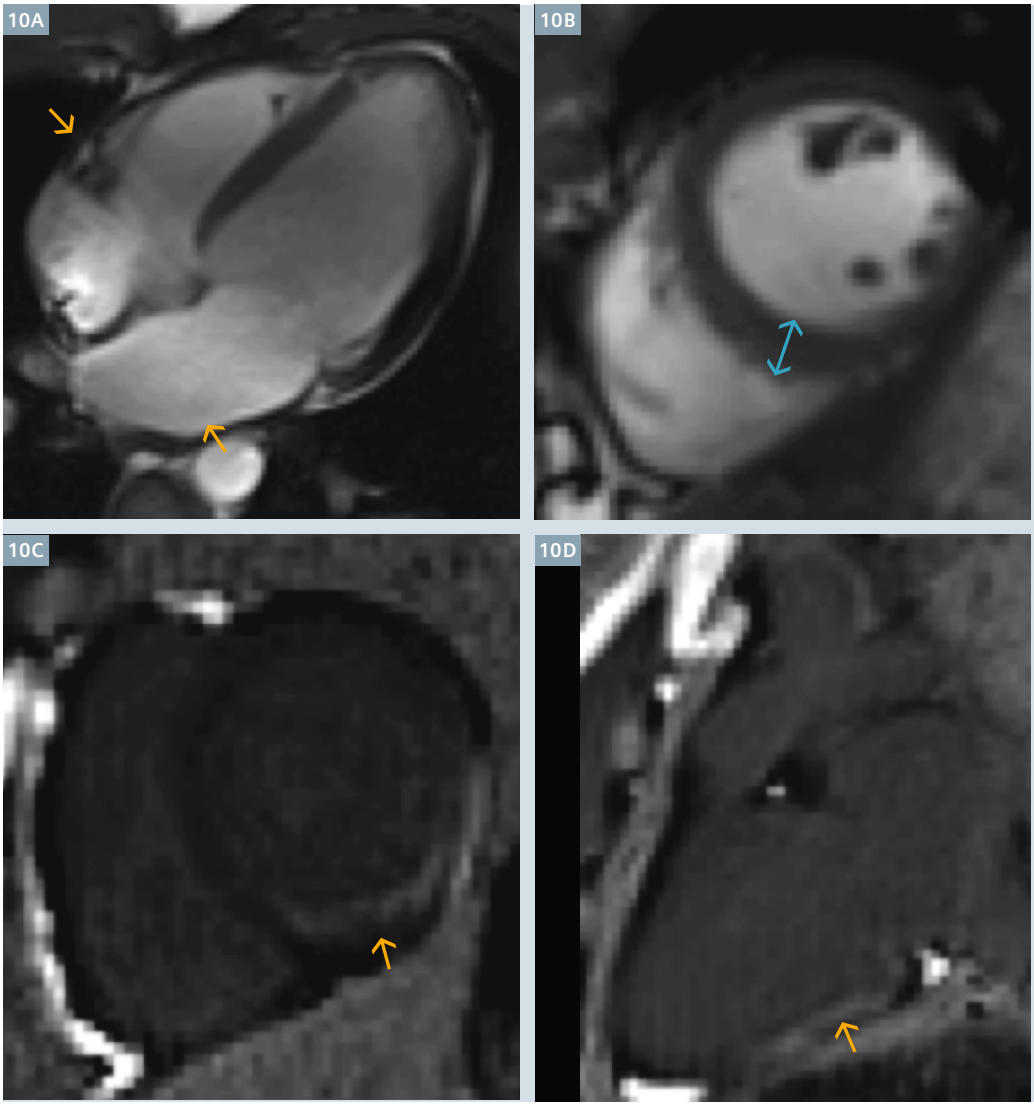

10 Preclinical HCM. Shown are images of a 35-year-old asymptomatic male patient with a family history of HCM.
(10A, B) SSFP sequential 4-chamber and short axis SSFP cine MR images reveal mid biatrial dilatation (thin yellow arrows) with no significant myocardial hypertrophy (double headed blue arrows).

(10C, D) PSIR images acquired 15 minutes post Gd administration reveal LGE along the inferior and posterior walls suggestive of early fibrosis.

entities. Mass-like HCM more precisely parallels the homogenous signal intensity characteristics and perfusion of adjacent normal myocardium, while tumors show heterogeneous signal intensity, enhancement, and perfusion characteristics that differ from those of remainder of the left ventricle [20].

6) Pre-clinical HCM

Screening of family members of patients with HCM is important because first-degree relatives of such patients have a 50% chance of being a gene carrier.

Cardiac MRI is a useful screening tool in patients with a normal LV thickness who have symptoms of HCM or in asymptomatic HCM mutation carriers. However, disease expression can be heterogenous and varied, even with the same mutation; hence follow-up screening needs to be considered every 2 to 5 years, particularly in young patients [20].

Figure 10 illustrates CMR finding s in a 36-year-old asymptomatic male patient with a family history of HCM.

Dilated cardiomyopathy (DCM)

These are a common cause of congestive heart failure characterized by fibrosis and decreased number of

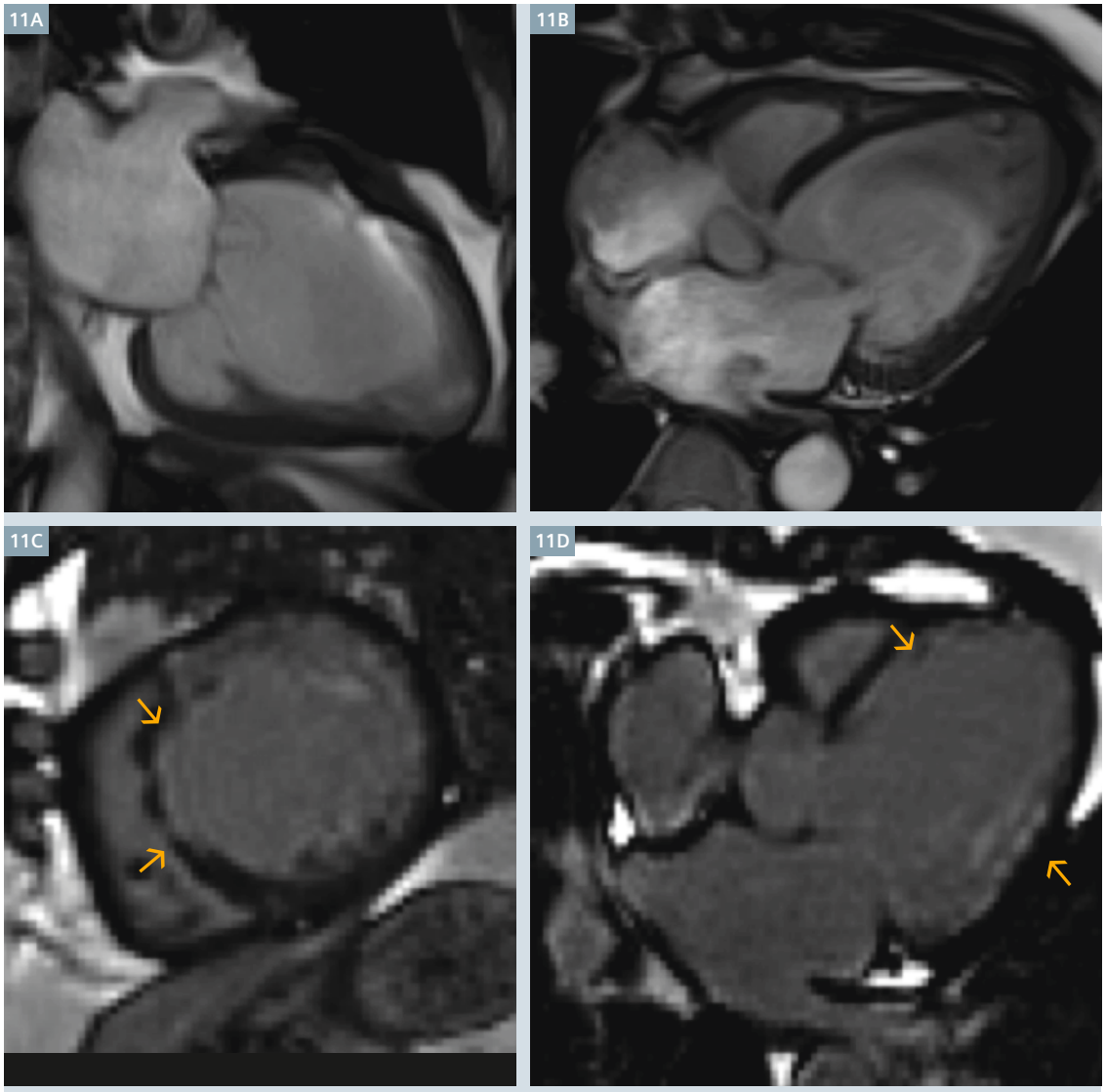

11 CMR of a 65-year-old male patient with a history of anterior wall MI.
(11A, B) SSFP 4- and 2-chamber chamber views reveal moderately dilated left ventricle.
(11B, C) PSIR images acquired 15 minutes post Gd administration reveals transmural LGE in the antero-septal wall, suggestive of non-viable myocardium in the LAD and RCA territories (thin yellow arrows).
The patient was diagnosed as ischaemic dilated cardiomyopathy.

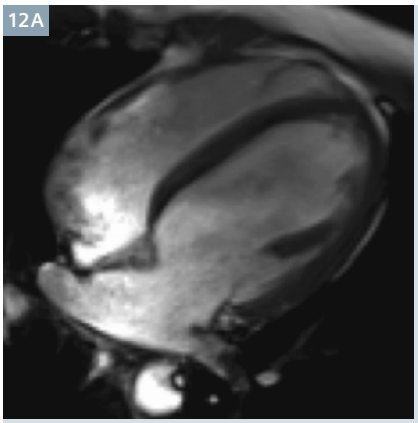

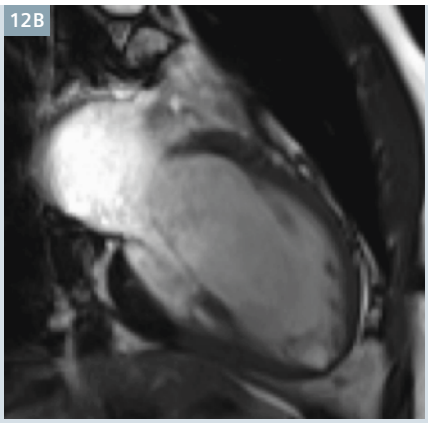

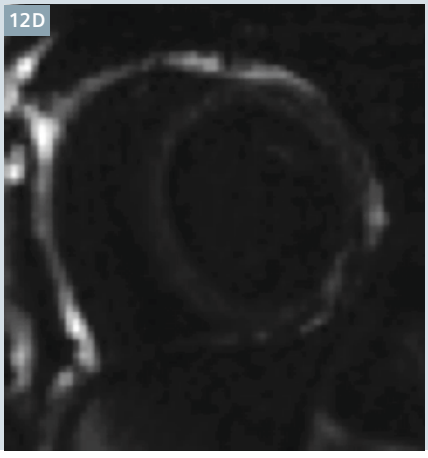

12

21-year-old male patient with complaints of progressive dyspnoea since childhood was referred for CMR.
(12A, B) SSFP 4- and 2-chamber views reveal moderate cardiomegaly.

(12C, D) PSIR images acquired 15 minutes post Gd administration reveal no LGE in the myocardium to suggest fibrosis. The patient was diagnosed as idiopathic/non ischaemic dilated cardiomyopathy.

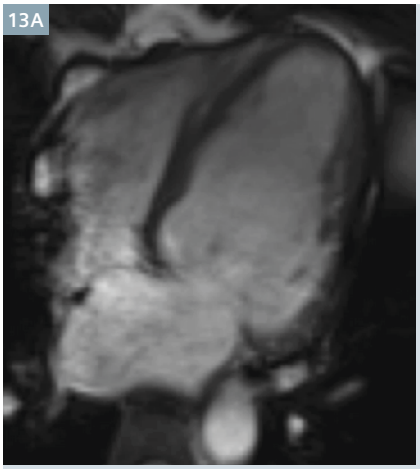

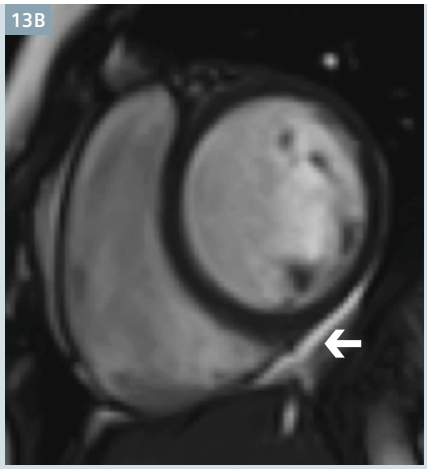

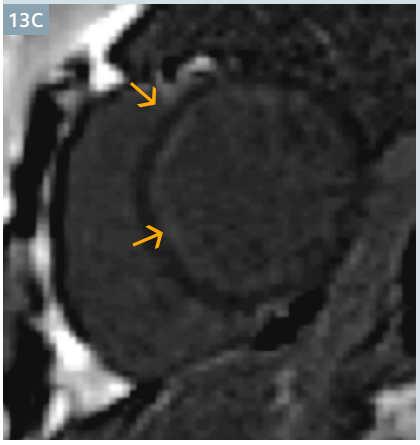

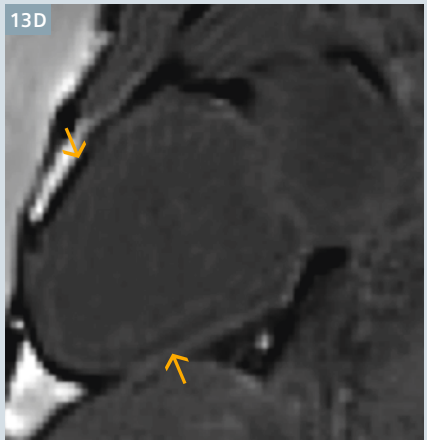

13

Example of an advanced case of idiopathic dilated cardiomyopathy in a 34-year-old female patient with dyspnoea and intermittent chest pain.
(13A, B) SSFP 4- and 2-chamber views respectively, show dilatation of all the cardiac chambers.

(13C, D) PSIR images acquired 15 minutes post Gd administration reveal diffuse subendocardial LGE in the septal, anterior and posterior walls (thin yellow arrows). Mild pericardial effusion can be appreciated on the short axis view (white solid arrow).

myocytes. The abnormalities seen in primary dilated cardiomyopathies are fairly similar to those seen as an end result of CAD (ischemic cardiomyopathy) [7]. LGE can be seen in both entities. However, ischemic injury progresses as a wavefront from the subendocardium to epicardium and shows a territorial distribution (Fig. 11). Hyper-enhancement patterns that spare the subendocardium and are limited to middle or epicardial portions of the LV, are clearly in a non-CAD distribution [9] (Fig. 12).

Restrictive cardiomyopathy

Restrictive CMP is characterised by reduced ventricular filling and diastolic volume, leading to atrial dilatation and venous stasis, with preserved systolic function. Restrictive CMP may be idiopathic, secondary to infiltrative and storage disorders (such as amyloidosis and sarcoidosis) or associated with myocardial disorders such as hypereosinophilic syndrome.

Cardiac MRI is a fundamental diagnostic tool because it helps in differentiating between restrictive CMP and constrictive pericarditis which have different therapeutic approaches. Although reduced ventricular filling and diastolic volumes may be a feature of both, pericardial thickening > 4 mm is typical of pericarditis [12] (Fig. 5).

Cardiac MRI also helps in the differentiation between the above entities in cases with minimally thickened pericardium. Morphologic images in restrictive CMP may show atrial enlargement. Cine images allow assessment of altered diastolic ventricular filling. Cine MRI assessment of diastolic ventricular septal movements and real time MRI imaging of septal movements during respiration show that in restrictive CMP, septal convexity is maintained in all respiratory phases, whereas in constrictive pericarditis, septal flattening can be seen in early inspiration [12] (Fig. 6). The issue of LGE in idiopathic restrictive CMP has not been specifically addressed in the literature, although late enhancement patterns in specific causes of restrictive CMP have been described [12].

Figure 14 illustrates a case of Restrictive CMP.

Non-compaction cardiomyopathy

Left ventricular myocardial non compaction (LVNC) is a recently recognised form of primary and genetic cardiomyopathy. Also known as spongy myocardium, LVNC is characterised by prominent ventricular myocardial trabeculations and deep intertrabecular recesses communicating with the ventricular cavity. LVNC is secondary to arrest in the normal process of myocardial compaction during fetal life.

CMR can clearly display the compacted and non-compacted myocardium layers better than echocardiography [13].

In a normal ventricle, the proportion of ventricular wall formed by trabeculations never exceeds thickness of the compacted layer. In LVNC, the thickness of non-compact myocardium is greater than that of compacted layer which is thinned. It is suggested that a NC/C ratio > 2.3 in diastole distinguishes pathological non compaction from pronounced trabeculae seen in other CMPs [13].

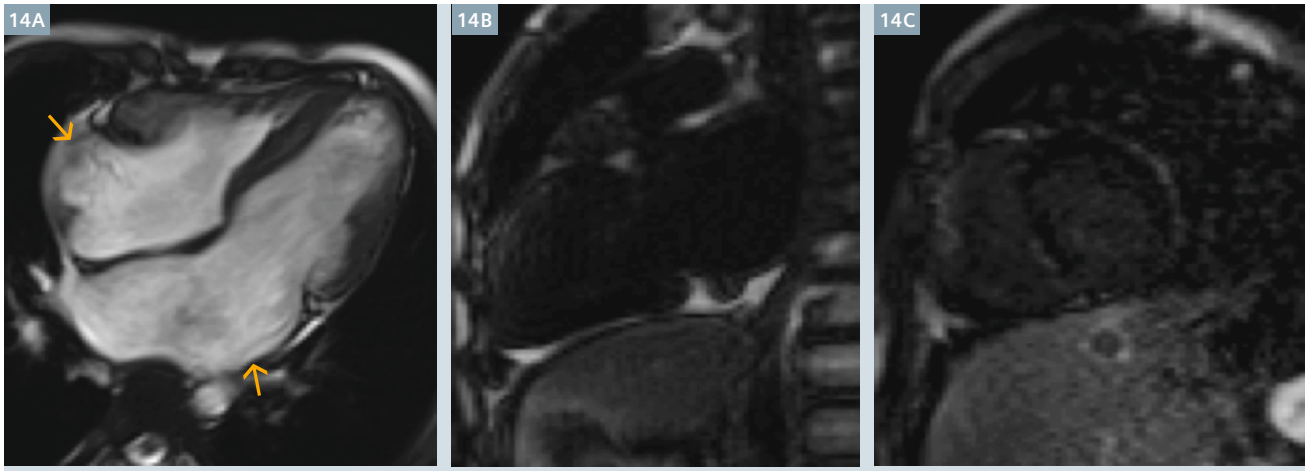

14 13-year-old female patient with a history of progressive dyspnoea.
(14A) SSFP images in the horizontal long axis view reveals significant bi-atrial dilatation (thin yellow arrows) with normal sized ventricular cavities.
(14B, C) PSIR images acquired 15 minutes post Gd administration demonstrate no enhancement in the myocardium.
Findings were suggestive of restrictive cardiomyopathy.

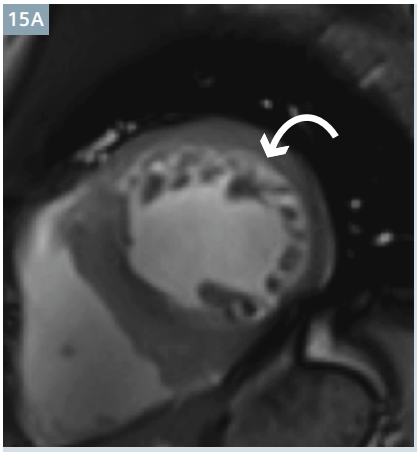

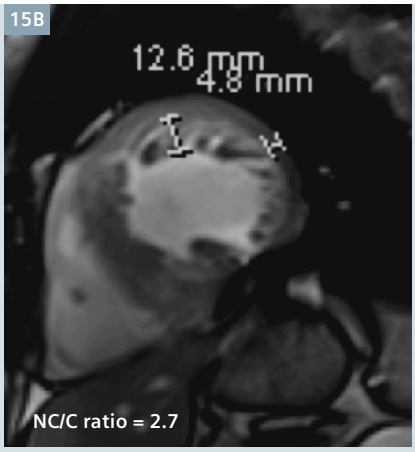

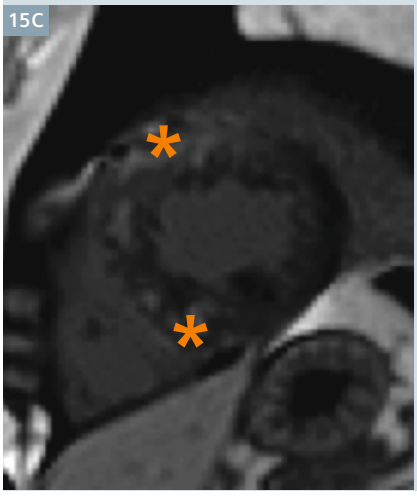

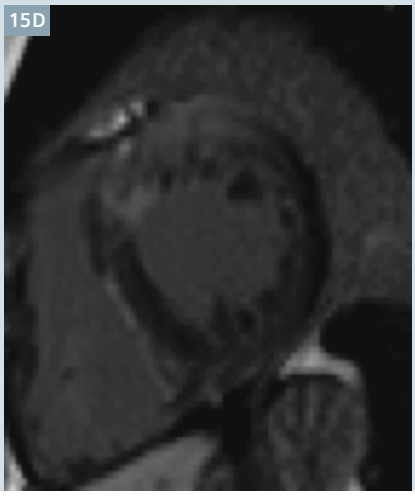

15

46-year-old asymptomatic male patient with a family history of sudden cardiac deaths came to our institution for CMR evaluation.
(15A, B) SSFP short axis images reveal severe non-compaction of the apex, mid lateral and mid anterior walls with a ratio of NC/C being 2.7 suggestive of non-compaction CMP. Left atrial dilatation was also observed.

(15C, D) PSIR images acquired 15 minutes after Gd administration showed moderate patchy LGE involving the anterior wall and interventricular septum, predominantly at the RV insertion sites (asterisk in C).

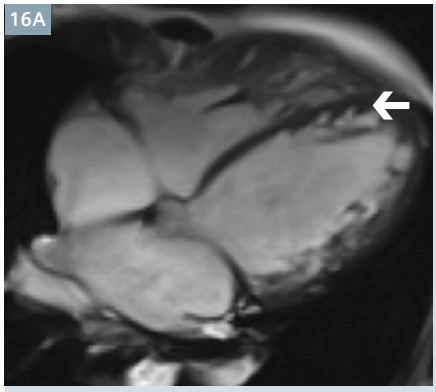

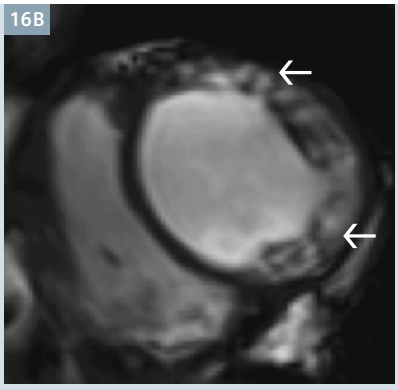

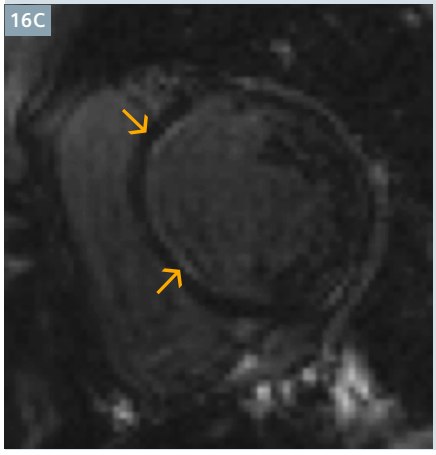

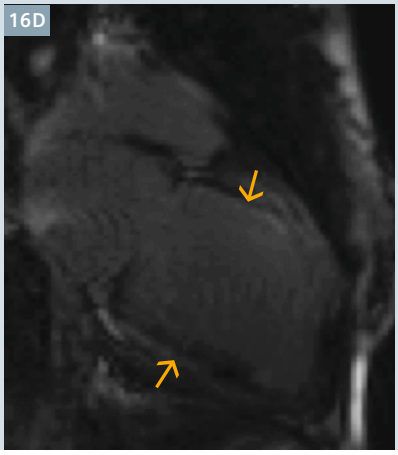

16

Another case of non-compaction CMP in a 28-year-old post-partum female with mild dyspnoea on exertion.
(16A, B) SSFP 4-chamber view and short axis images reveal moderate cardio-megaly with non-compaction seen along the lateral, inferior and posterior walls and the apex (white solid arrows).

(16C, D) PSIR images acquired 15 minutes post Gd administration reveal mild subendocardial LGE in the septal region, anterior and posterior walls, not conforming to any vascular territory (thin yellow arrows).

Figures 15, 16 demonstrate the imaging characteristics in non-compaction CMP.

Cardiac masses

CMR is widely recognised as the imaging modality of choice in evaluation of cardiac masses. Invasion in to adjacent structures, precise compartmental localisation can be easily accomplished narrowing the differential diagnosis [9].

1) ***Thrombus:*** a common differential diagnosis for cardiac tumors is intracardiac thrombus.

   Thrombi may appear isointense or slightly hyperintense relative to the myocardium on black blood prepared HASTE images [21] .Contrast-enhanced MRI enables differentiation between thrombus and surrounding myocardium as thrombus being avascular is characterized by lack of contrast uptake. Rarely, large chronic thrombi may show peripheral enhancement and be diagnostically challenging [17].

   Figure 17 shows a case of a patient suspected to have a LV clot (on echocardiography), confirmed on CMR.

2) ***Cardiac myxomas:*** These account for 20–25% of cardiac tumors. The most common locations are in the left atrium (60–75%), right atrium (20–28%), but rarely in both the atria and ventricles [17].

   Their contours are round or oval, sometimes lobulated with a smooth surface and a narrow pedicle. They have a gelatinous structure and may be relatively high in signal on SSFP and static images. They typically demonstrate heterogeneous enhancement on delayed-enhancement images [9] (Fig. 18).

   We encountered one patient referred for a CMR for assessment of a mass attached to the interventricular septum (as seen on echocardiography). Although the location was uncommon, the mass showed morphologic and enhancement characteristics of a myxoma and was diagnosed as such.

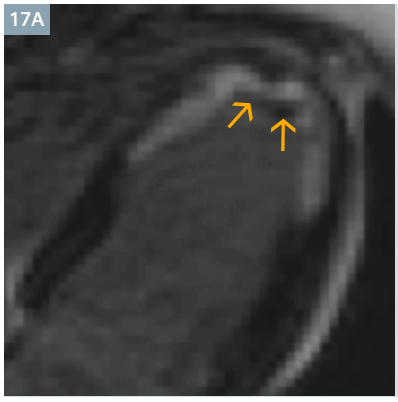

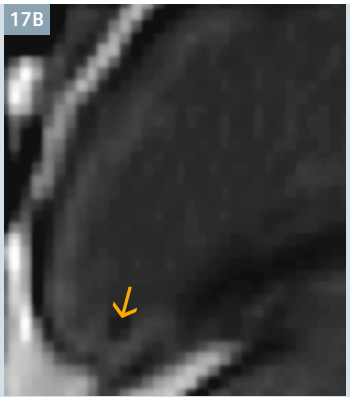

17

LV clots in a 65-year-old male patient with dyspnoea.
(17A, B) PSIR images acquired 15 minutes post Gd administration reveal transmural LGE in the apex and the anteroseptal wall suggestive of non-viable myocardium in the LAD. A layered non-enhancing clot is seen at the apex adjacent to the akinetic apical myocardium (thin yellow arrows).

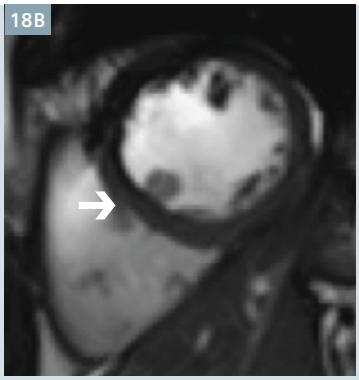

18

55-year-old male patient with a history of recurrent TIAs for CMR evaluation.
(18A, B) SSFP 4-chamber and short axis views reveal a nodular soft tissue mass adherent to the IV septum (solid white arrows).

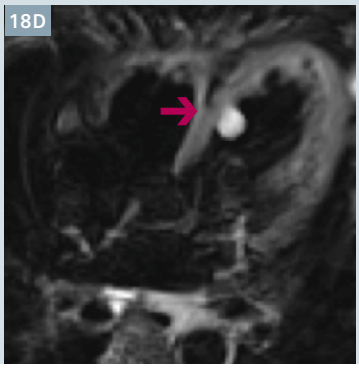

(18C, D) T1-weighted short axis and STIR 4-chamber views respectively demonstrate the mass which appears isointense to the myocardium on T1w and hyperintense on STIR images (myxoid content) suggestive of LV myxoma (solid red arrows).

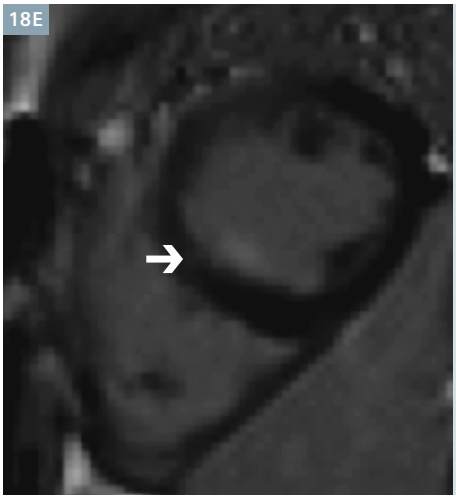

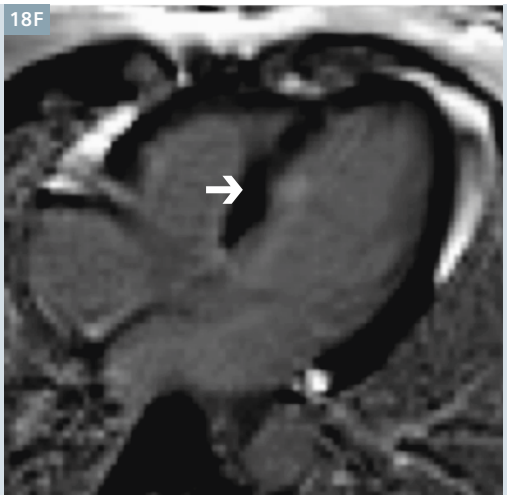

18

Contrast-enhanced study of the LV myxoma. **(18E, F)** PSIR images acquired 5 minutes and 15 minutes post Gd administration reveal minimal to no enhancement in the 5 min scan and intense homogenous enhancement in the delayed scan (solid white arrows).

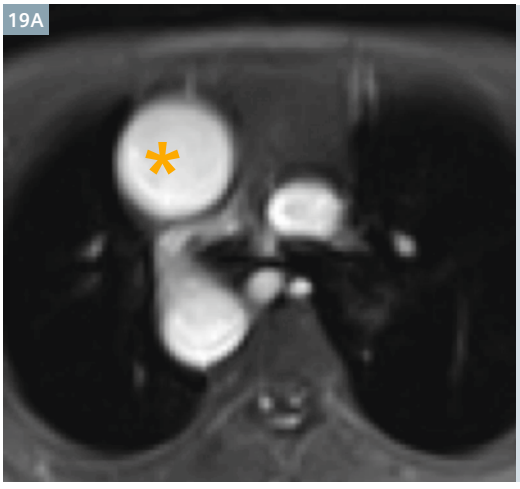

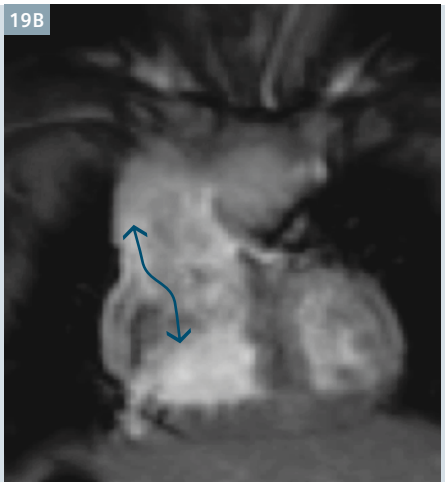

19

Figure **19A**: Shows right sided aortic arch (asterisk). **(19B)** Shows that the aorta arises from the morphological right ventricle (curved arrow).

Congenital heart diseases

Congenital heart disease is a common clinical entity and occurs in 0.8% of newborns [23]. Major advances in hardware design, new pulse sequences, and faster image reconstruction techniques allow rapid high resolution imaging of complex cardiovascular anatomy and physiology [24].

In our study, we imaged one 9-year-old male patient with complaints of progressive dyspnoea. Since contact of patients with CHDs referred for cardiac MRI exam is limited, we fragmented a single case of complicated CHD to demonstrate various cardiac anomalies.

The CMR study demonstrated the following cardiac anomalies:

- Ventricular septal defect: A common congenital heart disease classified into membranous, muscular, endocardial cushion defects, and conal [23] (Fig. 21A).
- Atroial septal defect: The main types of ASD are secundum (middle of atrial septum) as seen in figure 21B, sinus venosus (at junction of SVC and right atrium superiorly), and primum (near the AV valves) [23].
- Patent ductus arteriosus: PDA is the persistence of the 6th aortic arch and accounts for 10% of congenital heart disease. MRI demonstrates a persistent connection between the origin of left pulmonary artery to the descending aorta just beyond origin of the left subclavian artery [23] as seen in figure 22.
- Transposition of great arteries: The most common congenital heart lesion found in neonates, found in 5–7% of congenital cardiac malformations. Congenitally-corrected transposition refers atrioventricular discordance, ventricular inversion transposition, and inversion of great arteries [25] (Fig. 19).

Also observed in the same patient was situs inversus as shown in figure 20.

Limitations

A few technical limitations we encountered during our study on a 3T MRI were:

- Inability to achieve optimal myocardial nulling: Optimal TI scout was not obtained in three of our patients despite repeated attempts
- Exaggerated flow artifacts: Flow artifacts seemed to be more pronounced in areas of turbulent blood flow.

These technical issues have been forwarded to the Siemens application team and are currently under review. The team has in the past overcome many technical challenges of cardiac

20 Coronal T2-weighted image shows liver situated on left side of the abdomen – situs inversus.

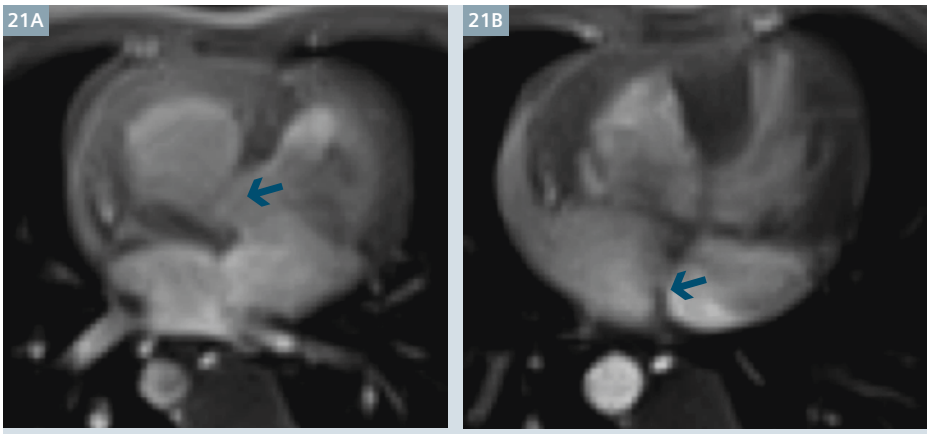

21 Figure **21A**: Shows ventricular septal defect (arrow). **(21B)** Shows atrial septal defect, secundum type (arrow).

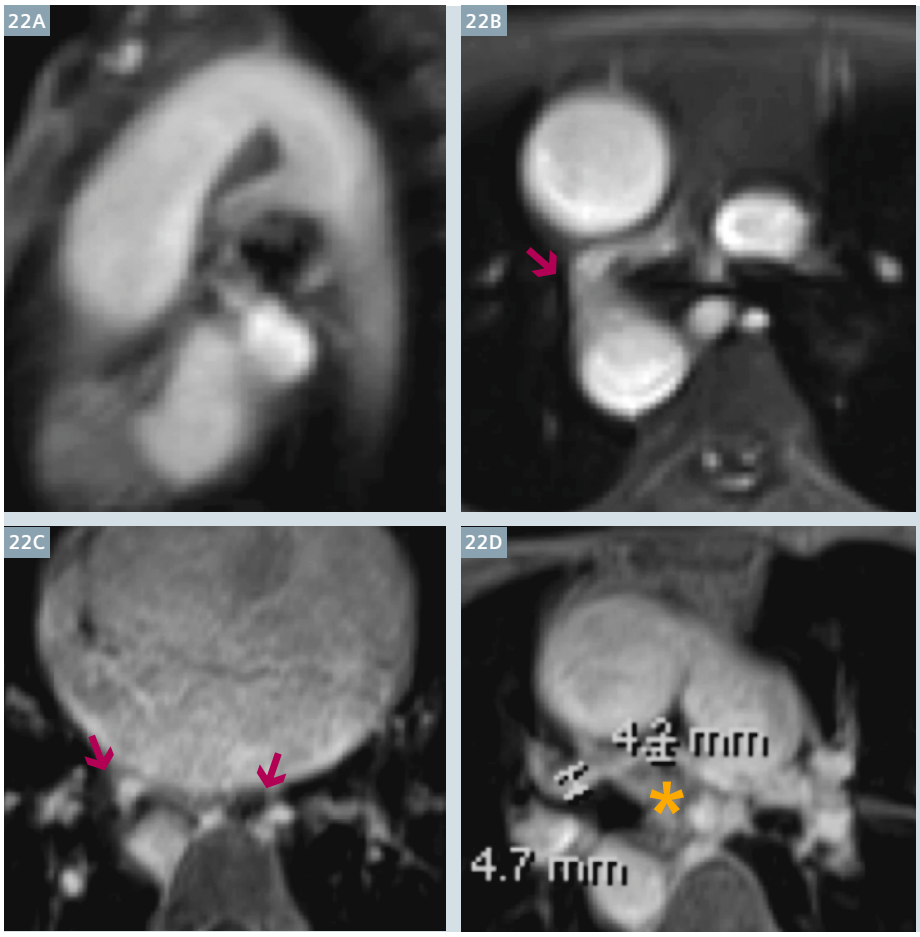

22 **(22A, B)** Demonstrate persistent ductus arteriosus (PDA) connecting aorta to pulmonary artery. **(22C)** Demonstrates multiple aortopulmonary collaterals (MAPCAs) (red arrows). **(22D)** Shows the atretic pulmonary trunks and main branch pulmonary arteries measuring 4 mm in diameter (yellow asterisk).

MRI on 3T due to high gradient factors in comparison with 1.5T, and optimized the protocol of cardiac MRI on 3T. With this experience, the team appears confident of being able to provide a solution to these limitations in the near future.

Conclusion

Cardiac MRI forms a mainstay investigation modality for a wide range of clinical applications and has emerged as a virtual 'one-stop' for imaging conditions like Cardiomyopathies [11]. CMR has added uniquely to the methods for non-invasive assessment of myocardial viability by a combination of cine imaging and delayed hyperenhancement (LGE).

CMR provides excellent depiction of pericardium in conditions such as pericarditis, pericardial effusions, and masses.

It provides optimal assessment of the location, functional characteristics, and soft tissue features of cardiac tumors, allowing accurate differentiation of benign and malignant lesions [17].

MRI is ideally suited to serve as the primary imaging modality in patients with congenital heart disease due its non-invasive and biologically harmless nature, and its ability to provide accurate anatomical and functional information [24].

Several investigators have confirmed the SNR advantages of CMR at 3T. These indicate an overall quantitative improvement in SNR and CNR, thus improving imaging capabilities. 3T protocols however, have not had time to be optimised in the way 1.5T have been in the past 10 years. Hence, simply using 1.5T protocols at 3T may not yield optimal imaging results [1]. More studies in the future are encouraged to standardise the protocols.

References

1 John N Oshinki, Jana G Delfino, Puneet Sharma, Ahmed M Gharib, Roderic I Pettigrew:Cardiovascular magnetic resonance at 3.0T: Current state of the art. Journal of Cardiovascular magnetic resonance2010, 12:55;1-13.

2 SCMR recommended Cardiac MRI Protocols; 1.5T and 3T Magnetom Systems with TIM and software version syngo MR 17.http://www.siemens.com/healthcare.

3 Roya S.Saleh, MD, Derek G. Lohan, MD, Kambiz Nael ,MD, Maleah Grover-Mckay, MD, and J.Paul Finn,MD: Cardiovascular MRI at 3T. APPLIED RADIOLOGY. Nov 2007; 10 to 26.

4 Ruth P. Lim, Monvadi B, Srichai and Vivian S. Lee; Non ischaemic causes of Delayed Myocardial hyperenhancement on MRI. American Journal of Radiology. June 2007; 188: 1675-1681.

5 The Radiology Assistant: Ischemic & non ischaemic cardiomyopathy. Radiology & Cardiology Department of the St. Antonius Hospital in Nieuwegein and the Rijnland Hospital in Leiderdorp, The Netherlands. http://www.radiologyassistant.nl/en/p4a3ff48cccc37/ischemic-and-non-ischemic-cardiomyopathy.html.

6 Louise E.J Thompson, MB ChB, Raymond J. Kim, MD, Robert M. Judd, PhD; Magnetic resonance imaging for assessment of myocardial viability: Journal of magnetic resonance imaging 19:771-788 (2004).

7 University of Virginia: Cardiac MRI: Cardiac MRI: The basics. Available from :https://www.med-ed.virginia.edu/courses/rad/cardiacmr/index.html.

8 A SEEGER, MD et al: MRI assessment of cardiac amyloidosis: experience of six cases with review of current literature. British Journal of Radiology. Apr 20009:337-342.

9 Grizzard et al. Cardiovascular MRI in practice, a teaching file approach. Springer; Nov 2008

10 Zhen F Wang, MD et al: CT and MR imaging of pericardial disease. RadioGraphics 2003; 23:S167–S180.

11 Priya Jagia, Gurpreet s Gulati, Sanjiv Sharma; Cardiac magnetic resonance in assessment of cardiomyopathies; Indian journal of radiology and imaging.MAY 2007;VOL 17:Issue 2: 109-119.

12 Elena Belloni et al; MRI of cardiomyopathy, December 2008,volume 191,Issue 6; 1702-1710.

13) FP Junqueira MD, FBD Fernandes MD, AC Coutinhojr MD, PV De Pontes MD, RC Dominques MD; Isolated left ventricular myocardial non-compaction: MR imaging findings from three cases. British Journal of Radiology, 82(2009), e37-e41.

14 Hua Gua, PhD; Myocardial T2 quantitation in patients with iron overload in 3T; J Magn Reson imaging.2009 August 30(2); 394-400.

15 John C. Wood; Impact of Iron Assessment by MRI; Strategies for Optimal management in Thalassemia-Now and in the future. American Society of Hematology, 2011:443-450.

16 Pippa Storey PhD;R2* imaging of transfusional iron burden at 3T and comparison with 1.5T; J Magn Reson imaging. 2007 March; 25(3): 540-547.

17 David H. O'Donell; Cardiac tumors: Optimal Cardiac MR sequences and Spectrum of Imaging appearences; American journal of Roentgenology; August 2009, volume 193; 377-387.

18 Mark W Hansen and Naeem Merchant: MRI of hypertrophic Cardiomyopathy: Part I, MRI appearances. American Journal of Radiology. December 2007, Volume 189; Issue 6.

19 Prabhakar Rajiah: Cardiac MRI part II-pericardial diseases. American Journal of Radiology Dec 27 2010: 197: W621-W634.

20 Eun Fu Chun, MD: Hypertrophic cardiomyopathy: Assessment with MR imaging and multidetector CT; Radiographics 2010; 30: 1309-1328.

21 Jorg Barkhausen et al; Detection and Characterisation of Intracardiac thrombi on MR imaging. American Journal of Radiology. May 2002; 179: 1539-1544.

22 Daniel M. Sodo, Jonathan M. Hasleton, Anna S Herry, & James C. Moon: CMR in heart failure.SAGE-Hindawi Access to Research. Cardiology Research & Practice. Vol 2011, Article ID 739157.

23 MN Sree Ram, CM Sreedhar, A Alam, IK Indrajit: The Role of Cardiac MRI in congenital heart disease: Indian Journal of Radiology and Imaging. 2005;vol 15,issue:2: 239-246.

24 Tal Geva, Davis J Sahn, Andrew J Powell;Magnetic resonance imaging of congenital heart disease in adults: Progress in Pediatric cardiology 17(2003): 21-39.

25 Emma C Ferguson, MD, Rajesh Krishnamurthy, MD and Sandra A.A. Oldham, MD, FACR; Classic Imaging Signs Of Congenital Cardiovascular Abnormalities; Radiographics September 2007,27: 1323-1334.

From left to right: Dr. Nikhil Kamat, Dr. M.L Rokade, Dr. Shubra Gupta, Dr. Kalashree Bidarkar and Rajesh Kamble (MRI technician)

Contact

Dr. Kalashree A.Bidarkar
Jupiter Hospital
Eastern Express Highway
Thane, Maharashtra
India
kalarad@gmail.com

Dr.Nikhil Kamat
Jupiter Hospital
Eastern Express Highway
Thane, Maharashtra
India
nikhilkamat1000@gmail.com